NIH Public Access
Author Manuscript
J Bone Miner Res. Author manuscript; available in PMC 2007 February 13.

Published in final edited form as:
J Bone Miner Res. 2006 March ; 21(3): 466–476.

Glucocorticoid-Treated Mice Have Localized Changes in Trabecular Bone Material Properties and Osteocyte Lacunar Size That Are Not Observed in Placebo-Treated or Estrogen-Deficient Mice

Nancy E Lane[1], **Wei Yao**[1], **Mehdi Balooch**[1], **Ravi K Nalla**[2], **Guive Balooch**[3], **Stefan Habelitz**[3], **John H Kinney**[3], and **Lynda F Bonewald**[4]

1 *Department of Medicine, University of California at Davis, Sacramento, California, USA*

2 *Materials Science Division, Lawrence Berkeley National Laboratory, Berkeley, California, USA*

3 *Department of Preventive and Restorative Dental Sciences, University of California at San Francisco, San Francisco, California, USA*

4 *Department of Oral Biology, University of Missouri at Kansas City School of Dentistry, Kansas City, Missouri, USA*

Abstract

This study compares changes in bone microstructure in 6-month-old male GC-treated and female ovariectomized mice to their respective controls. In addition to a reduction in trabecular bone volume, GC treatment reduced bone mineral and elastic modulus of bone adjacent to osteocytes that was not observed in control mice nor estrogen-deficient mice. These microstructural changes in combination with the macro-structural changes could amplify the bone fragility in this metabolic bone disease.

Introduction—Patients with glucocorticoid (GC)-induced secondary osteoporosis tend to fracture at higher bone mineral densities than patients with postmenopausal osteoporosis. This suggests that GCs may alter bone material properties in addition to BMD and bone macrostructure.

Materials and Methods—Changes in trabecular bone structure, elastic modulus, and mineral to matrix ratio of the fifth lumbar vertebrae was assessed in prednisolone-treated mice and placebo-treated controls for comparison with estrogen-deficient mice and sham-operated controls. Compression testing of the third lumbar vertebrae was performed to assess whole bone strength.

Results—Significant reductions in trabecular bone volume and whole bone strength occurred in both prednisolone-treated and estrogen-deficient mice compared with controls after 21 days ($p < 0.05$). The average elastic modulus over the entire surface of each trabecula was similar in all the experimental groups. However, localized changes within the trabeculae in areas surrounding the osteocyte lacunae were observed only in the prednisolone-treated mice. The size of the osteocyte lacunae was increased, reduced elastic modulus around the lacunae was observed, and a “halo” of hypomineralized bone surrounding the lacunae was observed. This was associated with reduced (nearly 40%) mineral to matrix ratio determined by Raman microspectroscopy. These localized changes in elastic modulus and bone mineral to matrix ratio were not observed in the other three experimental groups.

Address reprint requests to: Nancy E Lane, MD, Department of Medicine, University of California at Davis Medical Center, 4800 2nd Avenue, Suite 2600, Sacramento, CA 95817, USA, E-mail: nancy.lane@ucdmc.ucdavis.edu

The authors state that they have no conflicts of interest.

NIH-PA Author Manuscript
NIH-PA Author Manuscript
NIH-PA Author Manuscript

NIH-PA Author Manuscript

NIH-PA Author Manuscript

NIH-PA Author Manuscript

Conclusions—Based on these results, it seems that GCs may have direct effects on osteocytes, resulting in a modification of their microenvironment. These changes, including an enlargement of their lacunar space and the generation of a surrounding sphere of hypomineralized bone, seem to produce highly localized changes in bone material properties that may influence fracture risk.

Keywords

glucocorticoids; mice; elastic modulus; mineralization; bone strength

INTRODUCTION

Glucocorticoid (GC) treatment is frequently associated with an increase in the riskof bone fracture, especially in the spinal vertebrae and the femoral head.[1–3] GCs alter bone metabolism, which in turn decreases BMD and affects trabecular bone architecture. These changes in trabecular bone architecture and BMD do not explain the observed increase in fracture risk, because individuals treated with GCs frequently experience bone fractures at higher BMDs than women with postmenopausal osteoporosis.[4,5]

The explanation for bone fragility in adults with either estrogen-deficient osteoporosis or GC-induced osteoporosis is that changes in bone remodeling are responsible for altered trabecular bone volume and architecture such that the bone can no longer resist load; therefore, fractures occur.[6,7] Indeed, iliac crest biopsies from patients with bone loss caused by estrogen deficiency show reductions in trabecular bone volume, trabecular number, and connectivity, and these are associated with an increase fracture risk.[6,8] Recently, biochemical markers of bone turnover have emerged as surrogate measures of bone remodeling activity at the bone surface that can predict fracture risk independent of bone mass.[9] Individuals with high levels of bone turnover markers and low BMD have a higher risk of fracture.[9] Postmenopausal women who take bone-active agents that reduce bone remodeling (e.g., bisphosphonates) and have reductions in bone turnover markers are protected against bone fracture whether caused by postmenopausal osteoporosis or GC-induced osteoporosis.[10–12]

Individuals treated with GCs also have alterations in bone remodeling.[2,6,13] These alterations in bone remodeling include an increase in bone resorption and suppression of bone formation such that reductions in trabecular bone mass and architecture occur, including reductions in trabecular thickness and trabecular number.[6,7,13–15] The mechanisms behind these changes have been proposed to be alterations in bone cell viability. GCs reduce the lifespan of osteoblasts and osteocytes through apoptosis while increasing osteoclast viability.[14,15] Whereas these proposed alterations in bone cell lifespan could explain the reduction in bone formation markers and trabecular bone architecture, neither of these observations completely explains the increased bone fragility observed in GC-induced osteoporosis that is not observed with postmenopausal osteoporosis.

Therefore, we hypothesized that in addition to its alteration of bone mass and trabecular bone architecture; GCs may also alter the localized material properties of trabecular bone, thereby increasing bone fragility. To test this hypothesis we evaluated the localized material properties of the trabecular bone from mice treated with prednisolone and placebo, estrogen-deficient ovariectomized mice, and sham-operated controls.

MATERIALS AND METHODS

Animals and experimental procedures

For the GC study, 6-month-old male Swiss-Webster mice were obtained from Charles River (San Jose, CA, USA). The mice were maintained on commercial rodent chow (22/5 Rodent

NIH-PA Author Manuscript

NIH-PA Author Manuscript

NIH-PA Author Manuscript

Diet; Teklad, Madison, WI, USA) available ad libitum with 0.95% calcium and 0.67% phosphate. Mice were housed in a room that was maintained at 70°F with a 12-h light/dark cycle. The mice were randomized by body weight into two groups with eight animals each. Slow release pellets (Innovative Research of American, Sarasota, FL, USA) of placebo or 1.4 mg/kg/day of prednisolone were administered for 21 days by subcutaneous implantation.[15]

For the estrogen deficiency study, 6-month-old Swiss-Webster female mice were obtained from Charles River. Animals were either sham-operated or ovariectomized (OVX) by the dorsal approach as previously described.[16,17] The animals were killed 21 days after surgery. All animals were treated according to the USDA animal care guidelines with the approval of the UCSF Committee on Animal Research.[16]

For all study animals, calcein (10 mg/kg, IP) was given 14 and 4 days before death to determine bone formation surface and rate. One day before death, the mice were housed in individual metabolic cages, and a fasting 24-h urine sample was collected. Serum samples were obtained during necropsy, and both the urine and serum samples were stored at −80°C before the assessment of biochemical markers of bone turnover. At necropsy, the mice were exsanguinated by cardiac puncture, and successful removal of the ovaries in the OVX group was confirmed by failure to detect ovarian tissue and marked atrophy of the uterine horns. At the time of death, the third and fifth lumbar vertebral body (LVB) and femurs were placed in 10% phosphate-buffered formalin for 24 h and transferred to 70% ethanol for μCT, bone histomorphometry, scanning probe microscopy, and cell apoptosis measurements.

Biochemical markers of bone turnover

Urinary levels of deoxypyridinoline cross-links and creatinine (DPD/Cr) were analyzed in duplicate using ELISA kits from Quidel (Mountain View, CA, USA). Serum levels of osteocalcin (OSC) were measured using a mouse sandwich ELISA kit from Biomedical Technologies (Stroughton, MA, USA). The manufacturer's protocols were followed, and all samples were assayed in duplicate. A standard curve was generated from each kit, and the absolute concentrations were extrapolated from the standard curve. The CVs for intra- and interassay measurements were <8% for DPD, Cr, and OSC,[16,17] which is similar to the manufacturer's reference.

μCT

The fifth lumbar vertebral body from each of the animals was scanned with a desktop MicroCT (μCT viva 40; Scanco Medical, Bassersdorf, Switzerland), with an isotropic resolution of 10.5 μm for the vertebral body in all three spatial dimensions.[18] The number of slices varied according to the size of the vertebrae, ranging from 300 to 400 slices per specimen for the vertebral body. The scans were initiated in the sagittal plane of the vertebral body, covering the entire cortical and trabecular bone of the vertebral body. The scanning was initiated from the left periosteal margin to the right periosteum. The sagittal plane was chosen instead of the axial plane because this position compensates for the irregularity of the growth plate. Therefore, secondary spongiosa was consistently selected, and the primary spiongiosa was excluded from analysis.

3-D trabecular structural parameters were measured directly, as previously described.[18] Mineralized bone was separated from bone marrow with a marching cube 3-D segmentation algorithm in which the grayscale images were segmented using a constrained Gaussian filter (sigma = 0.8, support = 1) to remove noise, and a fixed threshold (235 grayscale value for vertebrae) was used to extract the structure of the mineralized tissue. Bone volume (BV) was calculated using tetrahedrons corresponding to the enclosed volume of the triangulated surface. Total volume (TV) was the volume of the sample that was examined. A normalized index, BV/

NIH-PA Author Manuscript

NIH-PA Author Manuscript

NIH-PA Author Manuscript

TV, was used to compare samples of varying size. The methods used for calculating trabecular thickness (Tb.Th), trabecular separation (Tb.Sp), and trabecular number (Tb.N) have been described.[19]

Cortical thickness was expressed as the average cortical thickness of three sections. For the vertebral body, one section was the center section, and the other two sections were 20 sections or 320 μm lateral to the center section. Both cortexes were measured at the middle height of the vertebral body. These methods have been used and previously published by our research group.[16,17]

Bone histomorphometry

The fifth lumbar vertebral bodies were dehydrated in ethanol, embedded undecalcified in methylmethacrylate, and sectioned longitudinally with a Leica/Jung 2255 microtome at 4- and 8-μm-thick sections. Bone histomorphometry was performed using a semiautomatic image analysis Bioquant system (Bioquant Image Analysis Corp., Nashville, TN, USA) linked to a microscope equipped with transmitted and fluorescence light.[20,21]

A counting window, allowing measurement of the entire trabecular bone and bone marrow within the growth plate and cortex, was created for the histomorphometric analysis. Static measurements included total tissue area (T.Ar), bone area (B.Ar), and bone perimeter (B.Pm). Dynamic measurements included single- (sL.Pm) and double-labeled perimeter (dL.Pm), osteoid perimeter (O.Pm), and interlabel width (Ir.L.Wi). These indices were used to calculate bone volume (BV/TV), trabecular number (Tb.N), trabecular thickness (Tb.Th), trabecular separation (Tb.Sp), mineralizing surface (MS/BS), percentage of osteoclast surface (Oc.S), and mineral apposition rate (MAR). Surface-based bone formation rate (BFR/BS) was calculated by multiplying mineralizing surface (single-labeled surface/2 + double-labeled surface) by MAR according to Parfitt et al.[20,21] We have reported similar methodology in other experiments in our laboratory.[16,17,19]

Measurement of apoptosis in undecalcified bone sections

Osteocyte apoptosis assays were performed using the undecalcified bone sections. The sections were mounted, deplasticized, and incubated in 20 μg/ml of proteinase K in PBS for 15 minutes at room temperature. Apoptotic cells were detected using TUNEL technology by using an in situ cell detection kit, Peroxidase (POD; Roche Applied Science, Indianapolis, IN, USA). The sections were counter-stained with 1% methyl green. Negative controls were generated by omitting the TdT from the labeling mix. ApopTag positive controls were generated from weaned rat mammary tissue fixed in 10% formalin.[22] To calculate the percentage of osteocyte apoptosis, an average of 2000 ± 216 (SD) osteocytes were counted per vertebral bone section (this included all trabeculae in the section). The percentage of apoptotic osteocytes was expressed as the number of apoptotic osteocytes divided by the total number of osteocytes present per vertebral bone section. Only osteocytes within the trabeculae were assessed from this analysis. These methods are similar to those reported by Weinstein et al.[14,15,23,24]

Elastic modulus mapping by scanning probe microscopy

A force modulation technique, elastic modulus mapping (E), was used to quantitatively map dynamic nanomechanical properties across the surface of the individual trabeculae with high spatial resolution (~15 nm). Modulus maps in the form of scanning probe microscopy (SPM) images were acquired using the direct force modulation-operating mode of a TriboScope nanoindenter (Hysitron, Minneapolis, MN, USA) mounted on a Multimode atomic force microscope (AFM) controlled by NanoScope IIIa electronics (Veeco, Santa Barbara, CA, USA).[25] For this experiment, the conventional AFM head was replaced by an electrostatic operated transducer that allowed for simultaneous topographic and elastic modulus imaging.

NIH-PA Author Manuscript

NIH-PA Author Manuscript

NIH-PA Author Manuscript

The electrostatic force acting on the spring-suspended center plate of the force–displacement transducer of the nanoindenter was sinusoidally modulated at 200 Hz while contact mode imaging was conducted. A cube corner diamond tip was attached to this transducer. The amplitude and the phase of the resulting transducer displacement signal were measured with a dual-channel lock-in amplifier. This information was used to determine the local indentation moduli of the sample at each pixel in the imaging process. The tip contact radius was determined by calibration using a quartz sample with known 69.7-GPa elastic modulus. When the tip was examined by scanning electron microscopy, the resulting tip radius was in good agreement (90%) with this calibration radius.[25]

To prepare the specimens for E, the methylmethacrylate embedded lumbar vertebral bodies that had been used to generate sections for bone histomorphometry were further polished with different diamond pastes, from 10 to 0.1 μm in diameter, to obtain smooth surfaces. The measurements were performed on three randomly selected vertebral specimens per treatment group and on all of the trabeculae that were in the specimen, roughly 6–10 different trabeculae from each sample. The amplitude of the modulated electrostatic force was set to 0.5–1.0 μN to maintain a good signal-to-noise ratio, but sufficiently small to prevent plastic deformation of the sample. Voigt and Hertzian models were used to extract the elastic modulus map of 256 × 256 pixels from the amplitude and phase of displacements at each pixel.[25–28] The entire surface area of each trabecula was covered in a mosaic fashion by small-overlapping individual 50 × 50-μm scans. After obtaining the elastic modulus image for each trabecula, the images were separated into different zones based on the elastic modulus results. Statistical analyses of the variations in elastic moduli were performed both on the entire trabecula as well as the individual zones.

Determination of mineral to matrix ratios using Raman microspectroscopy

Raman microspectroscopy was used to determine the inorganic (mineral) to organic (matrix) ratio of trabecular bone tissue surrounding the osteocyte lacunae across one trabecula from all four experimental groups. Raman spectra and resulting images were recorded using monochromatic radiation emitted by a He-Ne laser (632.8 nm), operating at 20 mW on a HR 800 Raman spectrophotometer (JobinYvon, Horiba, France). With the confocal capability of the instrument, a laser beam spot of <1 μm was focused just below the surface to minimize the effect of possible surface contamination by the methylmethacrylate surrounding the bone.

The integrated area of the spectra obtained from the inorganic component, represented by PO_4^{-3} (920–980 cm^{-1}) band peaks (apatite), were compared with the organic component (matrix), represented by the amide I band peaks at 1650–1720 cm^{-1}. For the image acquisition, an area of 70 × 70 μm was scanned pixel-by-pixel with a step size of 1 μm and an acquisition time of 30 s. The matrix and mineral bands were obtained separately. All measurements were made systematically under the same conditions, using ~1 μm depth in laser penetration. The spectral processing of the data included the subtraction of the background luminescence from the total spectra using a 10-point polynomial. The area of the background-corrected PO_4^{-3} ν1 envelope (920–980 cm^{-1}), measured using vender-supplied software (JobinYvon), was used as a measure of the mineral content. The area of the background-corrected amide I band envelope (1650–1720 cm^{-1}) was used as a measure of the matrix content in the mineral/matrix ratio calculation.[29–31]

Lacunar size and volume measurement

We assessed lacunar size and volume by two different methods. The sizes of lacunae were estimated from the polished sections of trabecular bone using the same diamond tip used for the elastic modulus mapping. The lacunae with the largest areas were located and assumed to

NIH-PA Author Manuscript

NIH-PA Author Manuscript

NIH-PA Author Manuscript

be the closest approximation to the midcross section of a 3-D ellipsoidal lacuna. These methods are similar to those reported by other investigators.[32,33]

Biomechanical testing

After death, the third lumbar vertebrae were excised from all mice from each experimental group ($n = 8$ per group) immersed into saline, wrapped in gauze, and frozen at −20°C until compression tests were performed. The relevant cross-sectional dimensions and the height of the specimens were measured using an optical microscope with a 0.5-μm resolution (Olympus STM-UM Measuring Microscope; Olympus American, Melville, NY, USA), after which they were subjected to unconfined compression tests along the long axis of the third lumbar vertebra. The tests were performed using a mechanical test frame (ELF 3200; TEC, Minnetonka, MN, USA) with a cross-head displacement rate of 0.01 mm/s, and involved loading the samples to failure, whereas continuously recording the corresponding loads and displacements. P_{max}, defined as the maximum load used to compress the specimen was determined from the load–displacement curve. The compression strength was calculated by dividing P_{max} by the cross-sectional area of the specimen.[34] Compression modulus was determined from the stiffness, which is the slope of the elastic portion of the load–displacement curve.[34]

Statistical analysis

The group means and SD were calculated for all outcome variables. Statistical differences between the prednisolone-treated and control groups and OVX and sham-operated groups were analyzed using Student's *t*-test for continuous variables and χ^2 tests for dichotomous variables. The non-parametric Kruskal-Wallis test with posthoc comparisons (SPSS Version 10; SPSS, Chicago, IL, USA) was used to assess the differences in elastic modulus and osteocyte lacunae size across the vertebral trabeculae in the placebo, prednisolone, sham-operated, and OVX mice. In all analyses, a priori, $p < 0.05$ was considered statistically significant.

RESULTS

General observations

The animals tolerated the surgery and the implantation of the pellets without complications. The mice implanted with prednisolone pellets had a modest weight loss over the first 7 days of the study (10% below baseline) but regained weight such that there were no differences in weights at day 21 between prednisolone- and placebo-treated animals. The mice that were OVX or sham-operated and observed over 21 days had a weight increase of 14–21% over baseline values ($p < 0.05$ within groups); however, no significant differences between the two groups was observed at day 21.

Trabecular and cortical bone changes measured by μCT

At day 21, compared with the placebo-treated mice, total trabecular bone volume was 22% lower ($p < 0.05$) in the prednisolone-treated animals (Table 1). Although trabecular connectivity was on average 10% lower, trabecular number was 4% lower and trabecular thickness was 7% lower in the prednisolone-treated animals compared with the controls (no statistical difference). The cortical thickness was 15% lower in prednisolone-treated mice compared with the placebo ($p < 0.05$). Compared with the sham-operated mice, total trabecular bone volume was ~18% lower, trabecular connectivity was 12% lower, and trabecular number was 7% lower in OVX mice ($p < 0.05$).

Histomorphometric measurements

Prednisolone and placebo groups—At the fifth lumbar vertebrae, prednisolone treatment reduced trabecular bone volume by an average of 19%, trabecular thickness by 42%,

NIH-PA Author Manuscript

NIH-PA Author Manuscript

NIH-PA Author Manuscript

and increased trabecular spacing by 41% compared with the placebo-treated mice ($p < 0.05$). In addition, after 21 days of prednisolone treatment, measures of dynamic trabecular bone turnover, including Oc.S., were on average 113% higher, with significantly lower MS/BS (−31%) and BFR/BS (−80%) than the placebo-treated mice ($p < 0.05$; Table 2).

OVX and sham-operated groups—After 21 days of estrogen deficiency, there was significantly lower trabecular bone volume (−30%), trabecular number (−45%), and 32% higher trabecular spacing than the sham-operated animals ($p < 0.05$). In addition, differences were detected in dynamic trabecular bone turnover measurements, including a higher Oc.S. (+150%; $p < 0.05$) and lower MS/BS (−12%) and BFR/BS (36%) in the OVX animals compared with sham-operated mice ($p < 0.05$; Table 2).

Interestingly, in both the prednisolone-treated mice and OVX mice, Oc.S was elevated to a similar extent compared with their respective controls. However, the reductions in bone formation variables (MS/BS, MAR, and BRF/BS) were greater in prednisolone-treated animals compared with OVX animals, despite the sex differences.

Analysis of biochemical markers in response to treatments

Prednisone treatment effects on bone turnover—Bone resorption, measured at day 21 by determination of DPD/Cr cross-links, was 1.9-fold higher in prednisolone-treated animals compared with placebo ($p < 0.05$; Table 3). Bone formation, assessed indirectly at day 21 by determination of osteocalcin, was 25% lower in prednisolone-treated mice compared with placebo ($p < 0.05$).

Estrogen deficiency effects on bone turnover—Bone resorption, measured at day 21 by determination of DPD/Cr cross-links, was 2-fold higher ($p < 0.05$) in OVX animals compared with the sham-operated controls. Bone formation, measured indirectly at day 21 by determination of osteocalcin, was similar in the OVX and sham-operated controls. Interestingly, compared with the OVX group, animals treated with prednisolone had 1.5-fold higher DPD/Cr values. These results suggest that, even after considering sex differences in the experimental groups, prednisolone treatment altered bone remodeling to a greater degree than estrogen deficiency over a 21-day period.

Elastic modulus mapping of trabeculae

Elastic modulus was obtained for six to eight trabeculae from each of the three fifth lumbar vertebral specimens from each treatment group. The mean ± SD of elastic modulus (GPa) for the prednisolone-treated group was 23.2 ± 4.7 and 24.2 ± 5.7 for the placebo controls. In addition, the mean of elastic modulus for the OVX group was 24.8 ± 3.2 and 25.0 ± 3.4 for the sham-operated controls.

Figure 1 shows a representative sample of an elastic modulus map of a trabecula from a prednisolone-treated mouse (Fig. 1A), a placebo-treated mouse (Fig. 1B), an estrogen-deficient mouse (Fig. 1C), and a sham-treated mouse (Fig. 1D). In the color scheme shown, the darker color corresponds to lower values of elastic modulus E. The average trabecula was covered by 8700–10,000 points. As expected, there was reduced E along the perimeter of the trabeculae from remodeling, which was more prominent in the prednisolone-treated and estrogen-deficient specimens compared with the controls (Figs. 1A–1D). However, two additional observations were made in the prednisolone-treated mice that were not observed in the three other groups. First, there were circular zones or “halos” ~25 μm in radius surrounding a significant number of osteocyte lacunae with nearly 40% reduced E (~14 GPa). Second, there was a ring-type zone at the perimeter of the area with reduced E that exhibited a slightly higher value of E than the mean across the trabeculae. Table 4 provides the percentage of osteocytes

NIH-PA Author Manuscript

NIH-PA Author Manuscript

NIH-PA Author Manuscript

that had reduced E (<20 GPa, or 30% reduced from the mean of the entire trabecula). There were nearly 20% of the total osteocytes in the prednisolone-treated group with reduced E surrounding the osteocytes compared with only 2–4% in the placebo and estrogen-deficient mice ($p < 0.05$). In addition, we quantified the reduced E along the edge of the trabeculae (<20 GPa, or 30% reduction from the mean of the trabecula) in each treatment group and found ~6.5% in the OVX group, 6.35% in the prednisolone-treated group, and essentially none in the placebo-treated or sham-operated groups.

Interestingly, we observed that the mean E across the entire trabeculae of the four experimental groups was similar, because the percentage of bone tissue around the osteocyte lacunae that changes with prednisolone treatment is small compared with total trabeculae area.

Raman microspectroscopy determination of mineral to matrix ratios

Figure 2 shows examples of a Raman image of amide I peaks (matrix) and phosphate peaks (major component of apatite) over methylmethacrylate (Fig. 2A) and around an osteocyte lacuna from a prednisolone-treated animal and a placebo-treated animal (Fig. 2B). The lower values are signified by the darker color. There is a loss of mineral as shown by a halo of the amide I (lower value) and phosphate (higher value) peaks around the osteocyte lacunae from the prednisolone-treated animals compared with the placebo group. To quantify the reduction in mineral surrounding the osteocyte lacunae, we determined the ratio of the background-corrected phosphate envelope to the background-corrected amide I envelope as plotted along a horizontal line in each sample evaluated (Fig. 2C). The mean value within the “halo” zone around the osteocyte lacuna in GC mice shows an ~30% reduction in mineral to matrix ratio from a normal value of ~7 in the placebo, estrogen-deficient, and sham-operated samples to a ratio of ~5 in the prednisolone-treated sample.

Quantification of osteocyte lacunae size and osteocyte apoptosis

We used the images obtained by SPM to calculate the cross-sectional area of the lacunae from three vertebral bone sections from four experimental groups (placebo, prednisolone, sham-operated, and OVX). The mean values and SD are shown in Table 4. The prednisolone-treated and OVX lacunae midsection areas are statistically larger than the placebo and sham-operated animals ($p < 0.05$), whereas prednisolone-treated lacunae were larger than OVX ($p < 0.05$). Assuming an ellipsoid shape, the lacunar volume were estimated as 402.4 μm^3 for placebo, 477.3 μm^3 for prednisolone-treated, 405.3 μm^3 for sham-operated, and 426.4 μm^3 for OVX samples.

Table 2 contains the quantitative data for osteocyte apoptosis. The percentage of apoptotic osteocytes assessed by the TUNEL assay was ~200% higher in prednisolone-treated mice compared with the placebo-treated mice ($p < 0.05$). There were no differences in percentage of apoptotic osteocytes in the OVX and sham-operated groups. However, the actual number of apoptotic osteocytes assessed in all of these experimental groups was low, <4% and 2% of the total osteocytes counted.

Biomechanical testing

At day 21, the third lumbar vertebra of mice treated with prednisolone had a 19% reduction in compression strength ($p < 0.05$) and 26% reduction in compression modulus ($p < 0.05$) compared with placebo-treated mice (Fig. 3). At day 21, OVX mice had a 17% reduction in strength ($p < .05$) and a 15% reduction in compression modulus ($p < 0.05$) compared with sham-operated mice. In general, damage was usually widespread in the compressed vertebrae; however, based on our observations, it seems that the damage initiates in the central section of the vertebra.

NIH-PA Author Manuscript

NIH-PA Author Manuscript

NIH-PA Author Manuscript

DISCUSSION

In this study, we observed that GC treatment focally altered the mechanical properties of the trabecular bone. There was a reduction in the elastic modulus both at the surface remodeling sites of the trabecular bone and around the osteocyte lacunae within the trabeculae. Whereas similar reductions in elastic modulus were observed at the trabecular surface of estrogen-deficient mice, the reduction of elastic modulus around the osteocyte lacunae was not seen in either the estrogen-deficient or the control mice. The reduction in elastic modulus surrounding the osteocyte lacunae was accompanied by a reduction in the mineral to matrix ratio. Similar to estrogen deficiency, changes in trabecular microarchitecture and whole bone strength occur, but unlike estrogen deficiency, changes in mechanical integrity surrounding osteocytes along with increased lacunar size are observed. These data suggest that GC-induced bone fragility occurs not only from changes in the trabecular microarchitecture but is compounded by changes in the local mechanical properties of the bone tissue itself.

Earlier studies have shown that GCs induce both osteoblast and osteocyte apoptosis in vitro and in vivo in both mice and humans.[14,15,23,24,35] Weinstein et al.[15] have found that GC treatment of mice resulted in reduced bone formation, increased bone resorption, and increased apoptosis of osteocytes and osteoblasts. We found greater numbers of apoptotic osteocytes in prednisolone-treated mice compared with the controls, but substantially less than reported by Weinstein et al.[14,25] Bellido et al.[36] reported in an in vitro study that GCs induced apoptosis of osteocytes. They assessed apoptosis with three different types of assays (trypan blue exclusion, nuclear morphology, and Annexin V/Propidium iodide ratios by fluorescence activated cell sorting [FACS] analysis) to accurately detect apoptosis and not nonprogrammed cell death. However, within bone slices, only the TUNEL assay can be used, and in this study, we may have missed the detection of some of the osteocytes within the prednisolone-treated bone undergoing apoptosis.

O'Brien et al.[23] reported prednisolone-treated mice had lower bone strength measured by compression testing of the fifth lumbar vertebrae than the control group. The major predictors of bone strength are total bone volume and architecture. Prednisolone-treated mice showed reductions in both total trabecular bone volume and trabecular thickness compared with the control group. In addition, the reduction in bone strength was similar between the prednisolone-treated mice and the estrogen-deficient mice, albeit the sex was different. Because both of these bone loss models have reductions in trabecular structure and bone mass of similar magnitude as their controls, we conclude that the loss of trabecular elements (e.g., number, thickness, or connections) was the most important element in the reduction in bone strength.[37] However, the alterations observed in the osteocyte microenvironment of demineralization with prednisolone treatment may contribute to the overall reduction in bone strength with prolonged periods of prednisolone exposure. Clinical studies of individuals on GCs have shown rapid bone loss occurring within a few months of initiating the therapy. Also, it seems that GC-treated subjects fracture at higher BMD values than postmenopausal women.[10] Therefore, both trabecular bone structural changes and localized changes within the trabeculae may contribute over time to increased bone fragility in GC-treated subjects.

In this study, we observed changes in elastic modulus surrounding osteocyte lacunae, reduced mineral to matrix ratios in the same areas, and an increase in lacunar size. This suggests that GCs may alter the metabolism and function of the osteocyte and is not just inducing cell death. It has been hypothesized that the osteocyte can remodel its local environment, which includes both the lacunae and canaliculi.[38] Osteocyte lacunae have been shown to uptake tetracycline, called "periosteocytic perilacunar tetracycline labeling," indicating the ability to calcify or form bone.[38] Alternatively, these investigators also found acid phosphatase–positive osteocytes near endosteal osteoclastic resorbing surfaces, suggesting potential capacity to

NIH-PA Author Manuscript

NIH-PA Author Manuscript

NIH-PA Author Manuscript

resorb. They also found greater solubility of the intralacunar mineral surrounding the normal osteocyte.[39] These observations suggest that the osteocyte can both add and remove mineral; our data support the latter.

In this study, we also observed larger osteocyte lacunae in prednisolone-treated mice compared with estrogen-deficient and control mice. The term “osteolytic osteolysis” was initially used to describe the enlarged lacunae in patients with hyperparathyroidism[40] and later in immobilized rats.[41] This term and concept became unfavored and was not used for more than two decades. This may be because of the fact that only enlargement and irregularity of the lacunae were the main morphological findings. Osteolytic osteolysis has been confused with the resorption mechanisms used by osteoclasts. Removal of mineral by osteocytes (weeks/months) would certainly be slower than osteoclastic resorption (days). Removal of mineral by osteocytes may involve a combined proteolytic (enzymes) and leaching (acid phosphatase) process. There are two ways that lacunar ultrastructure can be modified. One is by poor mineralization when the osteocyte is being formed. Bonucci and Gherardi[42] suggested this to be the reason for enlarged lacunae with renal osteodystrophy. In the case of our observations of decreased elastic modulus surrounding osteocyte in prednisolone-treated mice that was not observed in the placebo-treated animals, we postulate that the osteocyte modified the preexisting mineral of its surrounding matrix. The term “osteocyte halos” was used by Heuck[43] to describe pericanicular demineralization in rickets and later by others to describe periosteocytic lesions in X-linked hypophosphatemic rickets,[44] a condition caused by an inactivating mutation in Phex.[45] Such periosteocytic lesions are not present in other chronic hypophosphatemic states. The enlargement of the lacunar space in our study may be caused by similar or very different processes; however, the “leaching” of mineral from the surrounding mineralized matrix of the osteocyte resulted in the creation of a “halo” effect.

In this study, we used state-of-the-art technology to measure localized material properties of trabecular bone. However, there are also a number of shortcomings. We studied only one dose of prednisolone and one time-point, so we cannot generalize about dose response or time of exposure. In addition, it is not clear whether these changes persist, or whether remineralization occurs after cessation of prednisolone administration. These issues will be addressed in future experiments. Nevertheless, our observation that there are focal changes in tissue properties within the trabeculae, which would increase bone fragility, is consistent with clinical observations in which some patients treated with GCs suffer fractures at higher BMD values than in postmenopausal women.[4] Last, we performed our experiments in mice from two different sexes. Because GC-induced osteoporosis has been well validated in the male mouse model at 6 months of age, we chose to use this model. However, we do not think that the sex difference compromised our findings because both groups lost similar amounts of trabecular bone mass and whole bone strength during the 21-day experiment, and the differences we observed in the changes in elastic modulus and mineralization around the osteocyte in prednisolone-treated animals was not seen in any of the other three experimental groups.

In summary, our results suggest that prednisolone treatment altered localized material properties and bone matrix composition within the trabecula that was not observed in an estrogen-deficient mouse model. These localized changes, in addition to increased trabecular surface remodeling and trabecular bone structure deterioration, together may help to explain the excessive bone fragility observed in patients chronically treated with these medications.

Acknowledgements

This work was funded by NIH Grants R01 AR043052-07, R01 DK46661-10, and 1K24AR48841-02 and the Rosalind Russell Arthritis Research Center at UCSF and NIH PO1 AR46798 to LFB.

NIH-PA Author Manuscript

NIH-PA Author Manuscript

NIH-PA Author Manuscript

References

1. Lane NE. An update on glucocorticoid-induced osteoporosis. Rheum Dis Clin North Am 2001;27:235–254. [PubMed: 11285998]
2. Saag KG. Glucocorticoid-induced osteoporosis. Endocrinol Metab Clin North Am 2003;32:135–157. [PubMed: 12699296]
3. Cooper C, Coupland C, Mitchell M. Rheumatoid arthritis, corticosteroid therapy, and hip fracture. Ann Rheum Dis 1995;54:49–52. [PubMed: 7880122]
4. Van Staa TP, Laan RF, Barton IP, Cohen S, Reid DM, Cooper C. Bone density threshold and other predictors of vertebral fractures in patients receiving oral glucocorticoid therapy. Arthritis Rheum 2003;48:3224–3229. [PubMed: 14613287]
5. Van Staa TP, Leufkens HS, Cooper C. The epidemiology of corticosteroid osteoporosis. A meta-analysis. Osteoporos Int 2002;13:777–787. [PubMed: 12378366]
6. Dempster D. Iliac crest biopsy: Bone histomorphometry in glucocorticoid-induced osteoporosis. J Bone Miner Res 1989;4:137–141. [PubMed: 2658477]
7. Dalle Carbonare L, Arlot ME, Chavassieux PM, Roux JP, Portero NR, Meunier PJ. Comparison of trabecular bone architecture and remodeling in glucocorticoid-induced and postmenopausal osteoporosis. J Bone Miner Res 2001;16:97–103. [PubMed: 11149495]
8. Parfitt AM, Mathews CHE, Villanueva A, Kleerekoper M, Frame B, Rao DS. Relationships between surface, volume and thickness of iliac trabecular bone in aging and in osteoporosis. Implications for the microanatomic and cellular mechanisms of bone loss. J Clin Invest 1983;72:1396–1409. [PubMed: 6630513]
9. Garnero P, Hausherr E, Chapuy MC, Marcelli C, Grandjean H, Muller C, Cormier C, Breart G, Meunier PJ, Delmas PD. Markers of bone resorption predict hip fracture in elderly women: The EPIDOS Prospective Study. J Bone Miner Res 1996;11:1531–1538. [PubMed: 8889854]
10. Saag KG, Emkey R, Schnitzer TJ, Brown JP, Hawkins F, Goemaere S, Thamsborg G, Liberman UA, Delmas PD, Malice MP, Czachus M, Diafortis AG. Alendronate for the prevention and treatment of glucocorticoid-induced osteoporosis. N Engl J Med 1998;339:292–299. [PubMed: 9682041]
11. Bauer DC, Black DM, Garnero P, Hochberg M, Ott S, Orloff J, Thompson DE, Ewing SK, Delmas PD. Fracture Intervention Trial Study Group. Change in bone turnover and hip, non-spine, and vertebral fracture in alendronate-treated women: The fracture intervention trial. J Bone Miner Res 2004;19:1250–1258. [PubMed: 15231011]
12. Eastell R, Barton I, Hannon RA, Chines A, Garnero P, Delmas PD. Relationship of early changes in bone resorption to the reduction in fracture risk with risedronate. J Bone Miner Res 2003;18:1051–1056. [PubMed: 12817758]
13. Dovio A, Perazzolo L, Ostella G, Ventura M, Termine A, Milano E, Bertolotto A, Angeli AJ. Immediate fall of bone formation and transient increase of bone resorption in the course of high-dose, short-term glucocorticoid therapy in young patients with multiple sclerosis. Clin Endocrinol Metab 2004;89:4923–4928.
14. Manolagas SC, Weinstein RS. New developments in the pathogenesis and treatment of steroid-induced osteoporosis. J Bone Miner Res 1999;14:1061–1066. [PubMed: 10404005]
15. Weinstein RS, Jilka RL, Parfitt AM, Manolagas SC. Inhibition of osteoblastogenesis and promotion of apoptosis of osteoblasts and osteocytes by glucocorticoids. J Clin Invest 1998;102:274–282. [PubMed: 9664068]
16. Lane NE, Yao W, Kinney JH, Modin G, Balooch M, Wronski T. Both hPTH (1–34) and bFGF increase trabecular bone mass in osteopenic rats, however they have different effects on trabecular bone architecture. J Bone Miner Res 2003;18:2105–2115. [PubMed: 14672345]
17. Lane NE, Yao W, Nakamura MC, Humphrey MB, Kimmel D, Hunag X, Sheppard D, Ross FP, Teitelbaum SL. β5 Integrin deficiency increases osteoclast generation and activity and induces greater bone loss following ovariectomy. J Bone Miner Res 2005;20:58–66. [PubMed: 15619670]
18. Bouxsein ML, Uchiyama T, Rosen CJ, Shultz KL, Donahue LR, Turner CH, Sen S, Churchill GA, Muller R, Beamer WG. Mapping quantitative trait loci for vertebral trabecular bone volume fraction and microarchitecture in mice. J Bone Miner Res 2004;19:587–599. [PubMed: 15005846]

NIH-PA Author Manuscript

NIH-PA Author Manuscript

NIH-PA Author Manuscript

19. Humphrey MB, Ogasawara K, Yao W, Spusta SC, Daws MR, Lane NE, Lanier LL, Nakamura MC. The signaling adapter protein DAP12 regulates multinucleation during osteoclast development. J Bone Miner Res 2004;19:224–234. [PubMed: 14969392]
20. Parfitt AM, Drezner MK, Glorieux FH, Janis JA, Malluche H, Meunier PJ, Ott SM, Recker RR. Bone histomorphometry: Standardization of nomenclature, symbols and units. Report of the ASBMR Histomorphometry Committee. J Bone Miner Res 1987;2:595–610. [PubMed: 3455637]
21. Parfitt AM, Matthews CHE, Villanueva AR, Kleerekoper M, Frame B, Rao DS. Relationships between surface, area, and thickness of iliac trabecular bone in aging and in osteoporosis. J Clin Invest 1983;72:1396–1409. [PubMed: 6630513]
22. Ansari B, Coates PJ, Greenstein BD, Hall PA. In situ end-labelling detects DNA strand breaks in apoptosis and other physiological and pathological states. J Pathol 1993;170:1–8. [PubMed: 8326456]
23. O'Brien CA, Kai D, Plotkin LI, Bellido T, Powers CC, Stewart SA, Manolagas SC, Weinstein RS. Glucocorticoids act directly on osteoblasts and osteocytes to induce their apoptosis and reduce bone formation and strength. Endocrinology 2004;145:1835–1841. [PubMed: 14691012]
24. Weinstein RS, Chen J-R, Powers CC, Stewart SA, Landes RD, Bellido T, Parfitt AM, Manolagas SC. Promotion of osteoclast survival and antagonism of bisphosphonate induced osteoclast apoptosis by glucocorticoids. J Clin Invest 2002;109:1041–1048. [PubMed: 11956241]
25. Balooch G, Marshall GW, Marshall SJ, Warren OL, Asif SAS, Balooch M. Evaluation of a new modulus mapping technique to investigate microstructural features of human teeth. J Biomech 2004;37:1223–1232. [PubMed: 15212928]
26. Asif SAS, Wahl KJ, Colton RJ. Nanoindentation and contact stiffness measurement using force modulation with a capacitive load–displacement transducer. Rev Sci Instrum 1999;70:2408–2413.
27. Asif SAS, Wahl KJ, Colton R, Warren OL. Quantitative imaging of nanoscale mechanical properties using hybrid nanoindentation and force modulation. J Appl Phys 2001;90:1192–1200.
28. Kinney JH, Habelitz S, Marshall SJ, Marshall GW. The importance of intrafibrillar mineralization of the mechanical properties of dentin. J Dent Res 2004;82:957–961. [PubMed: 14630894]
29. Carden A, Morris MD. Application of vibrational spectroscopy to the study of mineralized tissues. J Biomed Opt 2000;5:259–268. [PubMed: 10958610]
30. Tarnowski C, Ignelzi MA Jr, Morris MD. Mineralization of developing mouse calaria as revealed by Raman microspectroscopy. J Bone Miner Res 2002;17:1118–1126. [PubMed: 12054168]
31. Ho SP, Balooch M, Marshall J, Marshall GW. Local properties of a functionally graded interphase between cementum and dentin. J Biomed Mater Res 2004;70A:480–489.
32. McCreadie BR, Hollister SJ, Schaller MB, Goldstein SA. Osteocyte lacuna size and shape in women with and without osteoporotic fracture. J Biomech 2004;27:563–572. [PubMed: 14996569]
33. Wright PH, Jowsey JO, Robb R. Osteocyte lacunae area in normal bone, hyperparathyroidism, renal disease, and osteoporosis. Surg Forum 1978;29:558–559. [PubMed: 401260]
34. Akhter AP, Cullen DM, Gong G, Recker R. Bone biomechanical properties in prostaglandin EP1 and EP2 knockout mice. Bone 2001;29:121–125. [PubMed: 11502472]
35. Tomkinson A, Reeve J, Shaw RW, Noble BS. The death of osteoclasts via apoptosis accompanies oestrogen withdrawal in human bone. J Clin Endocrinol Metab 1997;82:3128–3135. [PubMed: 9284757]
36. Ahuja S, Zhao S, Bellido T, Plotkin LI, Sato N, Bonewald LF. CD40 ligand blocks apoptosis induced by tumor necrosis factorí, glucocorticoids, and etoposide in the osteocyte-like cell line MLO-Y4. Endocrinology 2003;144:1761–1769. [PubMed: 12697681]
37. Deloffre P, Hans D, Rumelhart C, Mitton D, Tsouderso Y, Meunier PJ. Comparison between bone density and bone strength in glucocorticoid-treated aged ewes. Bone 1995;17:409S–414S. [PubMed: 8579945]
38. Baylink DJ, Wergedal JE. Bone formation by osteocytes. Am J Physiol 1971;221:669–678. [PubMed: 5570322]
39. Baylink, DJ.; Morey, E.; Rich, C. Effect of calcitonin on osteocyte mineral transfer in the rat. In: Talmage, R.; Belanger, L., editors. Parathyroid Hormone and Thyrocalcitonin. Excerpta Medical Foundation; Amsterdam, The Netherlands: 1968. p. 196-197.
40. Belanger LF. Osteocytic osteolysis. Calcif Tissue Res 1969;4:1–12. [PubMed: 4310125]

NIH-PA Author Manuscript

NIH-PA Author Manuscript

NIH-PA Author Manuscript

41. Kremlien B, Manegold C, Ritz E, Bommer J. The influence of immobilization on osteocyte morphology: Osteocyte differential count and electron microscopic studies. Virchows Arch A Pathol Anat Histol 1976;370:55–68. [PubMed: 818789]

42. Bonucci E, Gherardi G. Osteocyte ultrastructure in renal osteodystrophy. Virchows Arch A Pathol Anat Histol 1977;373:213–231. [PubMed: 140505]

43. Heuck F. Comparative investigations of the function of osteocytes on bone resorption. Calcif Tissue Res 1970;(Suppl 1):148–149. [PubMed: 5427962]

44. Marie PJ, Glorieux FH. Relation between hypomineralized periosteocytic lesions and bone mineralization in vitamin D-resistant rickets. Calcif Tissue Int 1983;35:443–448. [PubMed: 6311372]

45. Bai X, Miao D, Panda D, Grady S, McKee MD, Goltzman D, Karaplis AC. Partial rescue of the Hyp phenotype by osteoblast-targeted PHEX (phosphate-regulating gene with homologies to endopeptidases on the X chromosome) expression. Mol Endocrinol 2002;16:2913–2925. [PubMed: 12456809]

NIH-PA Author Manuscript

NIH-PA Author Manuscript

NIH-PA Author Manuscript

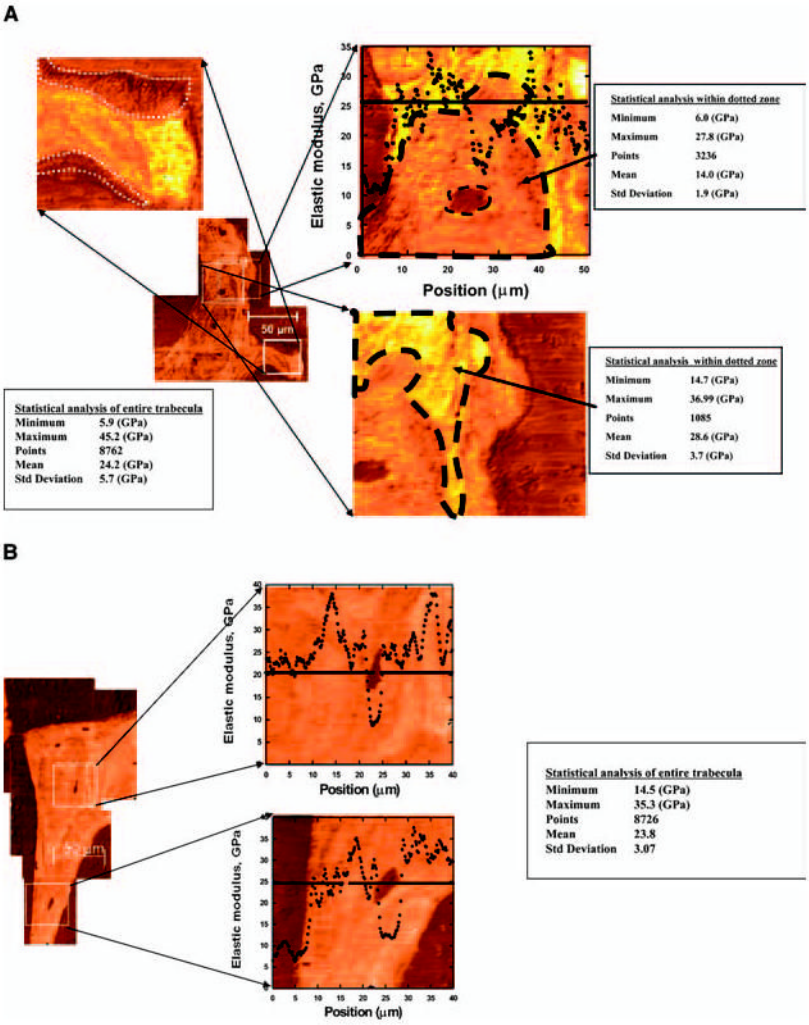

NIH-PA Author Manuscript
NIH-PA Author Manuscript
NIH-PA Author Manuscript

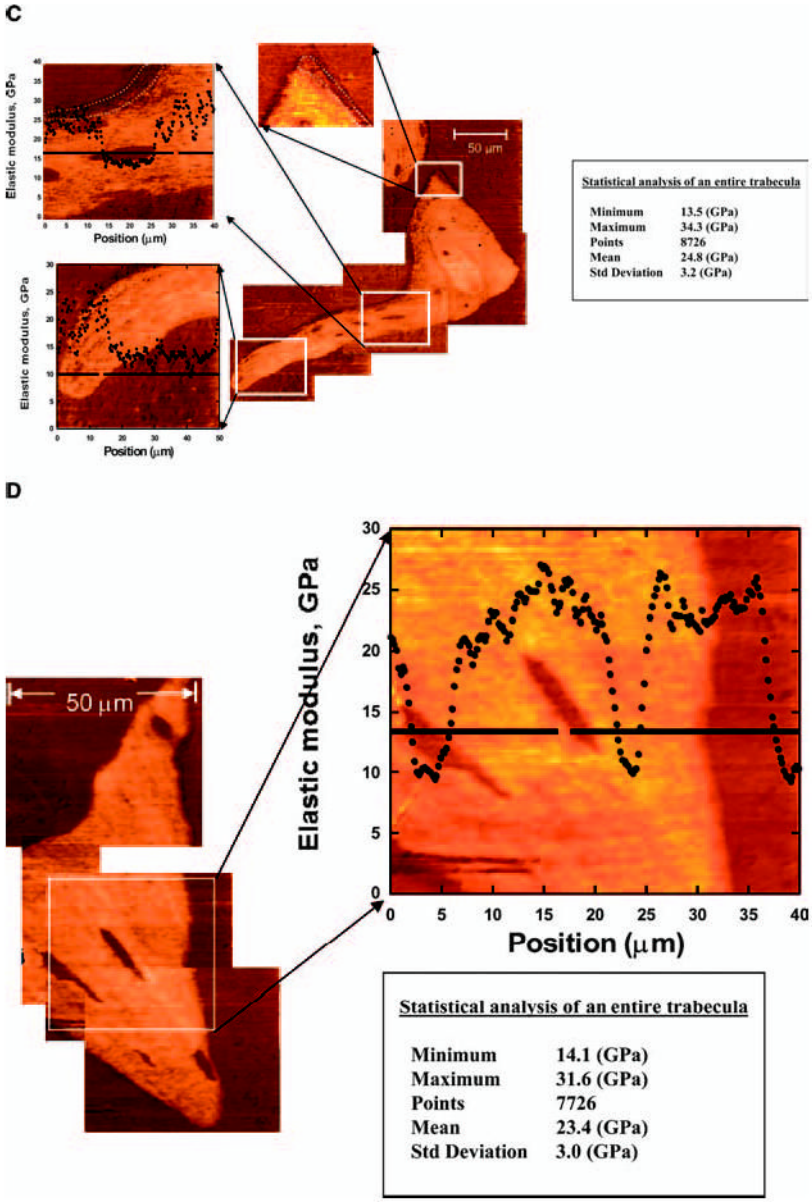

FIG. 1.

A representative sample of an elastic modulus map of an individual trabecula from four treatment groups is shown. Each figure represents a mean of >8000 points of data from each trabecula. (A) A trabecula from a prednisolone-treated mouse with a mean E of 24.2 ± 1.9 × 10^9 N/m^2 (GPa). A significant reduction in E (30% below the mean values) was observed at both the remodeling surface (shown within white dotted closed-loop lines) and around the osteocyte lacunae within the trabeculae (shown with black dotted closed-loop lines). (B) A trabecula from a placebo-treated male mouse showing a mean elastic modulus (E) of 23.8 ± 3.1 GPa with the expected reduction only over the osteocyte lacunae. (C) A trabecula from an ovariectomized mouse (after 21 days of estrogen deficiency) with a mean E of 24.8 ± 3.2 GPa, which was similar to the other study groups. E was reduced at the remodeling surface and over the osteocyte lacunae but not surrounding the osteocyte lacunae. (D) A sham-operated control with a mean E of 23.4 ± 3.0 GPa.

NIH-PA Author Manuscript
NIH-PA Author Manuscript
NIH-PA Author Manuscript

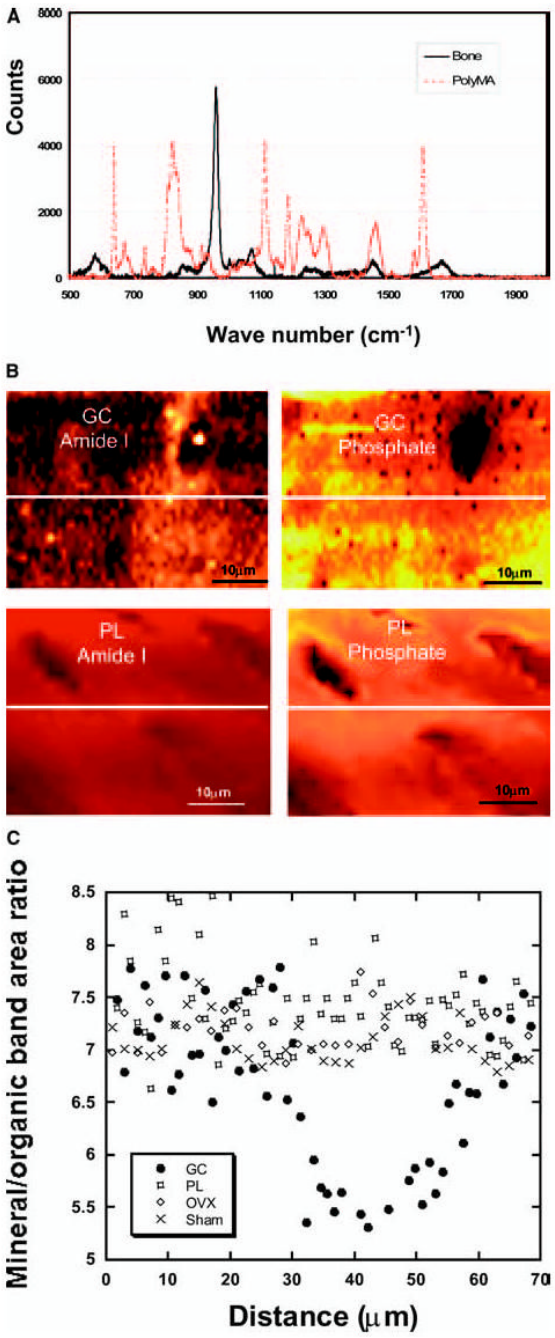

FIG. 2.

Raman microspectroscopic imaging of prednisolone-treated (GC) and placebo-treated (PL) mouse trabecula. (A) A comparison of the Raman spectrum of a typical bone embedded in methylmethacrylate and methylmethacrylate alone. (B) GC treatment reduces the mineralized tissue around the osteocyte lacunae and this is not seen in the PL-treated trabecula. (C) Quantitative mineral to organic band area ratios along the lines shown in B. There is a decrease in mineralized tissue (inorganic) to matrix (organic) peaks in mice treated with prednisolone. This change in the mineral to matrix ratio is not seen in the placebo-treated, sham-operated, or estrogen-deficient (OVX) mice (C).

NIH-PA Author Manuscript

NIH-PA Author Manuscript

NIH-PA Author Manuscript

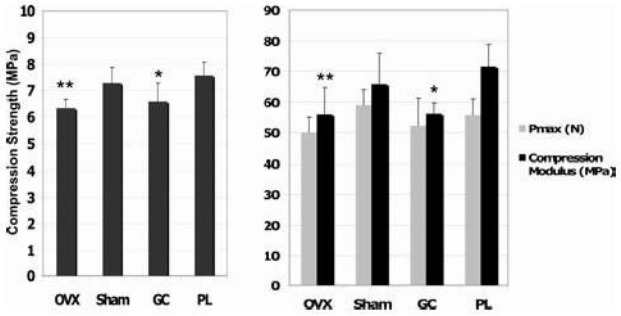

FIG. 3.

Biomechanical tests of the third lumbar vertebral body of mice from each treatment group (n = 8/group). Animals treated with prednisolone and estrogen-deficient mice have significant reductions in all measured mechanical property parameters compared with the control groups. P_{max} represents the maximum load measured in Newtons. *$p < 0.05$ from prednisolone-treated mice and **$p < 0.05$ from sham-operated mice.

NIH-PA Author Manuscript
NIH-PA Author Manuscript
NIH-PA Author Manuscript

Table 1

Trabecular and Cortical Bone Structural Variables of the Fifth Lumbar Vertebral Body Measured by μCT (Mean ± SD)

Treatment groups	Trabecular bone volume (%)	Trabecular connectivity ($1/mm^3$)	Trabecular number (1/mm)	Trabecular thickness (μm)	Cortical thickness (μm)
Distal femur					
1. Placebo	19.7 ± 1.6	206.8 ± 34.7	4.8 ± 0.5	50.7 ± 0.7	165.5 ± 32.5
2. Prednisolone	15.4 ± 2.9*	187.9 ± 80.6	4.6 ± 0.9	47.3 ± 0.8	139.9 ± 15.4*
3. Sham-operated	20.6 ± 4.3	184.4 ± 38.3	4.4 ± 0.5	47.9 ± 0.1	99.7 ± 14.0
4. OVX	16.9 ± 4.7†	162.7 ± 52.2†	4.1 ± 0.5†	43.7 ± 0.6	86.8 ± 13.6

Statistical tests were performed between groups 1 and 2 (prednisolone vs. placebo) and groups 3 and 4 (OVX vs. sham-operated).

* $p < 0.05$ from placebo.

† $p < 0.05$ from sham.

NIH-PA Author Manuscript NIH-PA Author Manuscript NIH-PA Author Manuscript

Table 2

Trabecular Bone Static and Dynamic Variables Assessed by Histomorphometry (Mean ± SD) and Number of Apoptotic Osteocytes (%) From the Fifth Lumbar Vertebral Body

Treatment groups	BV/TV (%)	Tb.N (1/mm)	Tb.Th. (μm)	Tb.Sp (μm)	Oc.S (%)	MS/BS (%)	MAR (μm)	BFR/BS ($\mu m^3/\mu m^2$/day)	Apoptosis osteocytes (%)
1. Placebo	17.9 ± 0.7	4.4 ± 0.5	24.9 ± 3.5	88.6 ± 10.0	0.8 ± 0.1	42.9 ± 12.9	1.03 ± 0.04	0.24 ± 0.05	1.9 ± 1.1
2. Prednisolone	14.5 ± 0.3*	4.0 ± 0.8	14.4 ± 4.0*	125.0 ± 17.8*	1.7 ± 0.4*	29.5 ± 6.5*	0.64 ± 0.07*	0.05 ± 0.01*	3.9 ± 1.0*
3. Sham-operated	18.6 ± 1.3	5.5 ± 1.1	28.5 ± 2.9	118.0 ± 11.0	1.3 ± 0.3	20.9 ± 8.8	0.90 ± 0.05	0.20 ± 0.16	1.0 ± 0.5
4. OVX	13.1 ± 4.4†	3.0 ± 0.8†	22.8 ± 6.0	156.4 ± 21.8†	3.3 ± 0.8†	23.4 ± 4.5	1.22 ± 0.11	0.28 ± 0.06	1.2 ± 0.6

Statistical tests were performed between groups 1 and 2 (prednisolone vs. placebo) and groups 3 and 4 (OVX vs. sham-operated).

* $p < 0.05$ from group 1.

† $p < 0.05$ from group 3.

NIH-PA Author Manuscript

NIH-PA Author Manuscript

NIH-PA Author Manuscript

Table 3

Biochemical Markers of Bone Turnover at Day 21 (Mean ± SD)

Groups	Deoxypyrinoline/Cr (nM/mM)	Osteocalcin (ng/ml)
Placebo	30.8 ± 7.9	99.5 ± 2.7
Prednisolone	59.3 ± 11.2*	75.2 ± 3.2*
Sham-operated	39.4 ± 3.2	70.8 ± 5.0
OVX	86.1 ± 37.7†	75.2 ± 2.0†

* $p < 0.05$ from placebo.

† $p < 0.05$ from sham-operated.

NIH-PA Author Manuscript

NIH-PA Author Manuscript

NIH-PA Author Manuscript

Table 4

Osteocyte Lacunae Size, Percentage of Osteocytes With Reduced Elastic Modulus Around the Perimeter of the Osteocyte Lacunae From the Four Experimental Groups (Mean ± SD)

Groups	No. of lacunae	Mean ± SD (μm^2)	Number (%)with reduced E (mean < 20 GPa) around osteocytes
1. Placebo	314	67.1 ± 5.1	10 (3%)
2. Prednisolone	385	91.8 ± 4.4*†	86 (22%)*†
3. Sham-operated	410	73.0 ± 5.0	7 (2%)
4. OVX	360	82.0 ± 4.3*	16 (4%)

* $p < 0.05$ from placebo and sham-operated mice.

† $p < 0.05$ from OVX.